MICROCOPY RESOLUTION TEST CHART

NATIONAL BUREAU OF STANDARDS 1963 A

AD-A190 736

OFFICE OF NAVAL RESEARCH

Anomalies in the Heat-Capacity Signatures of Submonolayer Adsorbates With
Attractive Lateral Interactions

by

Young Sik Kim, Franco Battaglia and Thomas F. George

Prepared for Publication

in

Journal of Chemical Physics

Departments of Chemistry and Physics
*State University of New York at Buffalo*
Buffalo, New York 14260

DTIC
ELECTE
FEB 1 8 1988
D

February 1988

88 2 17 007

# REPORT DOCUMENTATION PAGE

| 1a. REPORT SECURITY CLASSIFICATION Unclassified | | 1b. RESTRICTIVE MARKINGS | |
|---|---|---|---|
| 2a. SECURITY CLASSIFICATION AUTHORITY | | 3. DISTRIBUTION/AVAILABILITY OF REPORT Approved for public release; distribution unlimited | |
| 2b. DECLASSIFICATION/DOWNGRADING SCHEDULE | | | |
| 4. PERFORMING ORGANIZATION REPORT NUMBER(S) UBUFFALO/DC/88/TR-63 | | 5. MONITORING ORGANIZATION REPORT NUMBER(S) | |
| 6a. NAME OF PERFORMING ORGANIZATION Depts. Chemistry & Physics State University of New York | 6b. OFFICE SYMBOL (If applicable) | 7a. NAME OF MONITORING ORGANIZATION | |
| 6c. ADDRESS (City, State, and ZIP Code) Fronczak Hall, Amherst Campus Buffalo, New York 14260 | | 7b. ADDRESS (City, State, and ZIP Code) Chemistry Program 800 N. Quincy Street Arlington, Virginia 22217 | |
| 8a. NAME OF FUNDING/SPONSORING ORGANIZATION Office of Naval Research | 8b. OFFICE SYMBOL (If applicable) | 9. PROCUREMENT INSTRUMENT IDENTIFICATION NUMBER Contract N00014-86-K-0043 | |
| 8c. ADDRESS (City, State, and ZIP Code) Chemistry Program 800 N. Quincy Street Arlington, Virginia 22217 | | 10. SOURCE OF FUNDING NUMBERS | |

| | | 10. SOURCE OF FUNDING NUMBERS | | | |
|---|---|---|---|---|---|
| | | PROGRAM ELEMENT NO. | PROJECT NO. | TASK NO | WORK UNIT ACCESSION NO. |

**11. TITLE (Include Security Classification)**
Anomalies in the Heat-Capacity Signatures of Submonolayer Adsorbates with Attractive Lateral Interactions

**12. PERSONAL AUTHOR(S)** Young Sik Kim, Franco Battaglia and Thomas F. George

| 13a. TYPE OF REPORT | 13b. TIME COVERED FROM _____ TO _____ | 14. DATE OF REPORT (Year, Month, Day) February 1988 | 15. PAGE COUNT 20 |
|---|---|---|---|

**16. SUPPLEMENTARY NOTATION**
Prepared for publication in Journal of Chemical Physics

| 17. COSATI CODES | | | 18. SUBJECT TERMS (Continue on reverse if necessary and identify by block number) |
|---|---|---|---|
| FIELD | GROUP | SUB-GROUP | HEAT CAPACITIES, ANOMALIES, |
| | | | SUBMONOLAYER ADSORBATES, McQUISTAN-HOCK MODEL, |
| | | | ATTRACTIVE LATERAL INTERACTIONS, TWO-DIMENSIONAL LATTICE G |

**19. ABSTRACT (Continue on reverse if necessary and identify by block number)**

The analytic closed form of the heat-capacity signatures previously derived for the McQuistan-Hock (MQH) model of a lattice gas is applied to a various adsorbed systems for which the lateral interaction varies from a few meV to about 300 meV. It is shown that whenever the adsorption system can be described by a two-dimensional gas on which the substrate effects are less important than the adatom-adatom interactions, the computed temperatures at which the heat-capacity signatures display their maximum are in excellent agreement with the experimental measurements.

| 20. DISTRIBUTION/AVAILABILITY OF ABSTRACT ☒ UNCLASSIFIED/UNLIMITED ☒ SAME AS RPT. ☐ DTIC USERS | 21. ABSTRACT SECURITY CLASSIFICATION Unclassified | |
|---|---|---|
| 22a. NAME OF RESPONSIBLE INDIVIDUAL Dr. David L. Nelson | 22b. TELEPHONE (Include Area Code) (202) 696-4410 | 22c. OFFICE SYMBOL |

**DD Form 1473, JUN 86**     *Previous editions are obsolete.*     SECURITY CLASSIFICATION OF THIS PAGE

# LINE SHAPE OF AN ATOM-CRYSTAL BOND

Henk F. Arnoldus and Thomas F. George
Department of Physics
239 Fronczak Hall
State University of New York at Buffalo
Buffalo, New York 14260

## ABSTRACT

The spectral profile for the absorption of infrared laser light by a vibrational bond between a physisorbed atom and a harmonic crystal is calculated. We obtained an analytical expression for the line shape, which includes the finite memory-time effects in the interaction between atomic motion and bulk-atom vibrations. Both the memory in the time regression of the dipole correlation function and the initial correlations are taken into account. It is shown that absorption from a laser with a frequency which is larger than the cutoff frequency $\omega_D$ of the dispersion relation of the crystal can only occur due to a memory in the relaxation process, provided that multiphonon transitions are negligible. We predict a resonance-like line at $\omega_o + \omega_D$ (with $\omega_o$ the unperturbed resonance) for atom-surface bonds with a permanent dipole moment.

## I. INTRODUCTION

If a crystal is exposed to an atomic vapor, then many atoms will stick to its surface due to the van der Waals interaction. Every atom in the vicinity of the solid experiences an attractive potential, which supports continuum (desorbing) states and bound (adsorbing) states. Transitions from bound to continuum states can be induced by thermal coupling of the vibrational bond with the phonon reservoir of the crystal, or by illumination with a strong infrared laser. With the first mechanism a large desorption rate can be achieved by a sufficient heating of the substrate, whereas in the second process the transition to the continuum is brought about by photon absorption. For these processes the interaction between adsorbate and crystal can be accounted for by relaxation terms in a master equation for the populations of the vibrational levels, where the rate constants are given by the Golden Rule. Dynamical properties of the system are determined by the relative values of these rate constants and by the level structure of the potential. Then the desorption rate as a function of time contains information on the atom-crystal interaction, e.g. the rate constants. Several authors[1-3] applied this technique to evaluate the photodesorption yield as a function of the laser frequency. A far more sensitive method to obtain insight into the details of the dynamical features of adsorbates is by measuring the steady-state low-intensity absorption profile $I(\omega)$ as a function of the probe (laser) frequency $\omega$.[4-6] Then the absorption spectrum will reveal the details of dynamical atom-lattice bonds,[7] surface-modified internal molecular modes,[8] or properties of the interaction between two adspecies.[9] We shall consider a single atom which is adsorbed on a harmonic-lattice crystal, and bounded to the surface by a potential $V(z)$. We neglect lateral motion and indicate the normal to the surface by the z-axis. Then the induced dipole moment $\underline{\mu}(t)$, where t denotes the Heisenberg picture, of the atom-crystal bond must be in the z-direction, and hence

we can write $\underline{\mu}(t) = \mu(t)\underline{e}_z$ with $\mu(t)$ a scalar operator. An infrared laser with intensity $I_L$ (energy per unit of time which passes a unit surface area, perpendicular to the direction of propagation) and polarization $\underline{\epsilon}_L$ is incident on the atomic bond. Since the wavelength of the radiation is much larger than the atom-surface separation, we can adopt the dipole approximation for the interaction between the bond and the external field. Then a general expression for the absorbed energy per unit of time, the absorption profile, reads[10]

$$I(\omega) = I_L|\underline{e}_z \cdot \underline{\epsilon}_L|^2 \frac{\omega}{\epsilon_o \hbar c} \text{Re} \lim_{t \to \infty} \int_0^\infty d\tau \, e^{i\omega\tau} \text{Tr} \rho(t)[\mu(t+\tau), \mu(t)] \quad . \quad (1.1)$$

where $\rho(t)$ is the density operator for the atom, the entire crystal, and the interaction. The appearance of the commutator reflects that the net absorption is a balance between stimulated absorption (the term $\mu(t+\tau)\mu(t)$) and stimulated emission (the term $\mu(t)\mu(t+\tau)$) of photons from and into the laser field.

Transformation of Eq. (1.1) to the Schrödinger picture yields the equivalent expression

$$I(\omega) = I_L|\underline{e}_z \cdot \underline{\epsilon}_L|^2 \frac{\omega}{\epsilon_o \hbar c} \text{Re} \lim_{t \to \infty} \int_0^\infty d\tau \, \text{Tr} \mu e^{i(\omega-L)\tau}[\mu, \rho(t)] \quad . \quad (1.2)$$

Here, the limit $t \to \infty$ only pertains to the density operator $\rho(t)$, and obviously $\rho(t \to \infty)$ represents the thermal-equilibrium state of the system. If we write $\sigma$ for an arbitrary density operator, as we shall do throughout the paper, then the Liouvillian L in the exponential in Eq. (1.2) is related to the Hamiltonian H by

$$L\sigma = \hbar^{-1}[H, \sigma] \quad . \quad (1.3)$$

From Eq. (1.2) we notice that the frequency dependence of $I(\omega)$ is governed by the Fourier-Laplace parameter $\omega$ in the transformation of $\exp(-iL\tau)$, and consequently the resonance lines in the profile are situated at the eigenvalues of L. Then we recall that the equation of motion for the density operator is

$$i\,\frac{d\rho}{dt} = L\rho \quad , \tag{1.4}$$

and therefore the dynamical properties of the system will be displayed in the $\omega$-dependence of $I(\omega)$, even though the system is in a stationary state (for which $\rho(t)$ becomes independent of time). It is not the direct time evolution of $\rho(t)$ which is probed by the laser, but the time-regression operator $\exp(-iL\tau)$ of the dipole correlation functions, as they appear in Eq. (1.1). The significance of a measurement of $I(\omega)$ then relies on the fact that L represents the entire system, rather than only the vibrational bond.

## II. HAMILTONIAN

A harmonic crystal can be represented by the Hamiltonian $H_p$ for its phonon field[11]

$$H_p = \sum_{\underset{\sim}{k}s} \hbar\omega_s(\underset{\sim}{k}) a^{\dagger}_{\underset{\sim}{k}s} a_{\underset{\sim}{k}s} \quad , \tag{2.1}$$

in terms of the annihilation ($a_{\underset{\sim}{k}s}$) and creation ($a^{\dagger}_{\underset{\sim}{k}s}$) operators for phonons in the mode $\underset{\sim}{k}s$. Here, $\underset{\sim}{k}$ and $s$ denote the wave vectors and polarizations, respectively, and $\omega_s(\underset{\sim}{k})$ is the dispersion relation. The Hamiltonian for the bounded atom includes a kinetic energy and a potential

$$H_a = - \frac{\hbar}{2m} \frac{d^2}{dz^2} + V(z) \quad , \tag{2.2}$$

with $m$ the mass of the atom. Eigenstates and eigenvalues of $H_a$ can be found easily for a variety of potentials $V(z)$. An important example is the Morse potential, which models the atom-crystal binding quite accurately. Kinetic coupling between the atomic motion and the phonon field is assumed to be dominated by single-phonon interactions, for which the Hamiltonian reads

$$H_{ap} = -(\underline{u} \cdot \underline{e}_z) \frac{dV}{dz} \quad . \tag{2.3}$$

The operator $\underline{u}$ is the displacement of the crystal atom which is closest to the adsorbate. Explicitly[11]

$$\underline{u} = \sum_{\underline{k}s} \left( \frac{\hbar v}{2M V \omega_s(\underline{k})} \right)^{\frac{1}{2}} (a_{\underline{k}s} + a^{\dagger}_{-\underline{k}s}) \underline{e}_{\underline{k}s} \quad , \tag{2.4}$$

with $V$ and $v$ the volumes of the crystal and a unit cell, respectively, $M$ the mass of a crystal atom, and $\underline{e}_{\underline{k}s}$ the unit polarization vector of a phonon in the mode $\underline{k}s$. The total Hamiltonian then becomes

$$H = H_p + H_a + H_{ap} \quad , \tag{2.5}$$

which determines the Liouvillian $L$ according to Eq. (1.3). Then the density operator $\rho(t)$ of the system follows after solution of Eq. (1.4), and the spectral profile is obtained in evaluating expression (1.2).

## III.  RESERVOIR CORRELATION FUNCTION

Due to the many degrees of freedom of the phonon field a direct diagonalization of the Hamiltonian is intractable, so that we have to resort to an approximation.  The thermal-equilibrium density operator of the crystal at temperature T is

$$\bar{\rho}_p = \{Tr_p \exp(-H_p/k_B T)\}^{-1} \exp(-H_p/k_B T) \quad , \tag{3.1}$$

with $k_B$ Boltzmann's constant, and where $Tr_p$ indicates a trace over the states of the phonon field only.  Then the idea is that the large crystal can be regarded as a thermal reservoir, and that its state $\bar{\rho}_p$ is not affected by the presence of the single atom on the surface.  The central quantity in standard relaxation theory[12] is the reservoir correlation function

$$f(\tau) = \hbar^{-2} Tr_p (\underline{u} \cdot \underline{e}_z) e^{iL_p \tau} (\bar{\rho}_p \underline{u} \cdot \underline{e}_z) \quad , \tag{3.2}$$

with $L_p \sigma = [H_p, \sigma]/\hbar$.  Relaxation constants are then expressed in the Fourier-Laplace transform of $f(\tau)$

$$\tilde{f}(\omega) = \int_0^\infty d\tau \, e^{i\omega\tau} f(\tau) \quad . \tag{3.3}$$

We shall adopt a Debye model for the dispersion relation, which implies

$$\omega_s(\underline{k}) = c'k \, H(\omega_D - c'k) \quad , \tag{3.4}$$

in terms of the Debye frequency $\omega_D$, the speed of sound $c'$, and the unit-step function H. Furthermore, we recall the relation

$$\frac{v}{c'^3} = \frac{6\pi^2}{\omega_D^3} \quad ,$$

(3.5)

expressing that the cutoff frequency $\omega_D$ appears as a consequence of the finiteness of the volume v of a unit cell. Then it is an easy matter to compute $\tilde{f}(\omega)$, and we obtain[13]

$$\tilde{f}(\omega) = \xi \, g(\omega/\omega_D)$$

(3.6)

where the overall factor is given by

$$\xi = \frac{3\pi}{2\hbar M \omega_D^2} \quad .$$

(3.7)

The dimensionless function $g(\omega/\omega_D)$ which represents the $\omega$-dependence of $\tilde{f}(\omega)$ is found to be

$$g(z) = zH(z)H(1-z) - \frac{1}{\pi}\left(1+z\log\left|1-\frac{1}{z}\right|\right) + \frac{|z|}{e^{\gamma|z|}-1}H(1-|z|)$$

$$+ \frac{1}{\pi} \, P \int_0^1 dx \, \frac{1}{e^{\gamma x}-1} \times \frac{2zx}{z^2-x^2} \quad ,$$

(3.8)

which depends parametrically on the temperature through

$$\gamma = \frac{\hbar\omega_D}{k_B T} \quad .$$

(3.9)

It will appear that the function g(z) incorporates the refinements of an absorption line in comparison with the standard Lorentzian. A plot of g(z) can be found in Ref. 13.

Two important properties of g(z), which can be deduced from Eq. (3.8), are

$$\text{Re } g(z) = 0 \qquad \text{for} \quad |z| > 1 \ , \tag{3.10}$$

$$g(-z) = g(z)^* \qquad \text{for} \quad T \to \infty \ . \tag{3.11}$$

Furthermore, g(z) goes to zero very fast for $|z| > 1$. This implies, in view of Eq. (3.3), that $f(\tau)$ has a time width of the order of $1/\omega_D$. In a previous paper[14] we pointed out that this feature prohibits the application of the Markov approximation in the derivation of an equation for the reduced adsorbate density operator $\rho_a(t)$, defined by

$$\rho_a(t) = \text{Tr}_p \rho(t) \ . \tag{3.12}$$

If only a master equation for the populations of the vibrational states is of interest (as for instance in the desorption problem), then the finite time width of $f(\tau)$ does not have much significance, but for the evaluation of an absorption profile it is of paramount importance that the details of $\tilde{f}(\omega)$ are taken into consideration, as we shall show below.

## IV. DENSITY OPERATOR

Finite memory-time reservoir theory is a complicated mathematical tool, which can be applied to solve Eq. (1.4) for $\rho_a(t)$ and to evaluate steady-state quantum correlation functions, as they appear in Eq. (1.1). Recently we developed the

general theory,[15] and in this paper we apply the formalism to the computation of line shapes of adsorbates.

If we would be able to prepare the adsorbate at time zero in state $\rho_a(0)$, then its state for $t \geq 0$ is given by

$$\bar{\rho}_a(\omega) = \frac{i}{\omega - L_a + i\Gamma(\omega)} \rho_a(0) \qquad (4.1)$$

in the Fourier-Laplace domain. As usual, $L_a$ denotes the commutator with $H_a$, divided by $\hbar$. Coupling to the reservoir is embodied in the relaxation operator $\Gamma(\omega)$, defined by

$$\Gamma(\omega)\sigma_a = Tr_p L_{ap} \frac{i}{\omega - L_a - L_p} L_{ap}(\sigma_a \bar{\rho}_p) \quad , \qquad (4.2)$$

where $\sigma_a$ is an arbitrary adsorbate density operator, and $L_{ap}\rho = [H_{ap}, \rho]/\hbar$. The operator inversion on the right-hand side of Eq. (4.2) might seem awkward, but in Ref. 15 we have shown how to evaluate explicitly the matrix elements of $\Gamma(\omega)$.

For the steady-state line profile we only need the long-time solution of $\rho_a(t)$, which can be found from its Fourier-Laplace transform according to

$$\bar{\rho}_a = \lim_{t \to \infty} \rho_a(t) = \lim_{\omega \to 0} -i\omega \bar{\rho}_a(\omega) \quad . \qquad (4.3)$$

With Eq. (4.1) we then see that $\bar{\rho}_a$ is the solution of

$$(L_a - i\Gamma(0))\bar{\rho}_a = 0 \quad , \qquad (4.4)$$

and of course the restictions $\bar{\rho}_a^\dagger = \bar{\rho}_a$, $Tr_a \bar{\rho}_a = 1$ should be imposed.

In the Markov or zero memory-time approximation, the relaxation operator $\Gamma(\omega)$ acquires a frequency-independent value. It is the $\omega$-dependence of $\Gamma(\omega)$ which reflects the memory in the atom-crystal interaction. In the long-time limit the density operator is determined by $\Gamma(\omega)$ at $\omega = 0$, but this operator is not equal to its Markovian equivalent, as shown elsewhere.[14]

## V. ABSORPTION PROFILE

From Eq. (1.1) we notice that the absorption profile involves quantities as $\mathrm{Tr}\rho(t)\mu(t+\tau)\mu(t)$, which depend on two times, and their evaluation is correspondingly more complicated. In this section we derive a formal expression for $I(\omega)$.

First we introduce a two-time operator

$$D(\tau,t) = e^{-iL\tau}[\mu,\rho(t)] \tag{5.1}$$

and its Fourier-Laplace transform

$$\bar{D}(\omega,t) = \int_0^\infty d\tau \, e^{i\omega\tau} D(\tau,t) \quad, \tag{5.2}$$

where the frequency dependence only refers to the first argument of $D(\tau,t)$. We remark that $D(\tau,t)$ is an operator in the entire atom plus crystal Hilbert space. Comparison of Eqs. (5.1) and (5.2) with Eq. (1.2) shows that the expression for $I(\omega)$ can be cast in the form

$$I(\omega) = I_L |\underline{e}_z \cdot \underline{\epsilon}_L|^2 \frac{\omega}{\epsilon_0 \hbar c} \mathrm{Re} \lim_{t\to\infty} \mathrm{Tr}\mu\bar{D}(\omega,t) \quad. \tag{5.3}$$

From the fact that the dipole operator $\mu$ acts only on adsorbate states, it follows that

$$\text{Tr}\mu\tilde{D}(\omega,t) - \text{Tr}_a\mu\tilde{D}_a(\omega,t) \quad , \tag{5.4}$$

with $\tilde{D}_a(\omega,t) - \text{Tr}_p\tilde{D}(\omega,t)$, the reduced adsorbate operator.

Then we notice that $D(\tau,t)$ obeys

$$i\frac{d}{d\tau} D(\tau,t) - L\, D(\tau,t) \quad , \qquad \tau \geq 0 \quad , \tag{5.5}$$

as is evident from its definition (5.1). Hence the $\tau$-dependence of $D(\tau,t)$ is governed by the same equation as the one which determines the time evolution of the density operator $\rho(t)$, Eq. (1.4). An important difference is that the initial value for Eq. (5.5) reads

$$D(0,t) - [\mu,\rho(t)] \quad , \tag{5.6}$$

in contrast to the equation for $\rho(t)$, where $\rho(0)$ can be chosen arbitrarily. The time regression of $D(\tau,t)$ on the interval $0 < \tau < \infty$ is identical to the time evolution of $\rho(t)$ on $0 < t < \infty$, and therefore it should be possible to express $\tilde{D}(\omega,t)$ in $\Gamma(\omega)$. Additionally, the initial value $D(0,t)$ depends explicitly on t, via $\rho(t)$, and in a finite memory-time theory this quantity will carry a memory to the time evolution of $\rho(t)$ in the recent past (times smaller than t). Contributions to the line profile which arise due to this mechanism will be referred to as initial correlations. It might seem that in the limit $t \to \infty$ we can replace $\rho(t)$ by $\bar{\rho}_a\bar{\rho}_p$, which would eliminate initial correlations. We shall show that this is not correct in general. In Ref. 15 we have developed a general

method for the evaluation of quantities of the form $\bar{D}_a(\omega, t \to \infty)$. If we apply that theory to the present situation, we find the formal expression for the absorption profile

$$I(\omega) = I_L |\underline{e}_z \cdot \underline{\epsilon}_L|^2 \frac{\omega}{\epsilon_o \hbar c} \mathrm{Re} \mathrm{Tr}_a L_X \frac{i}{\omega - L_a + i\Gamma(\omega)} (L_Y - iT(\omega)) \bar{\rho}_a \quad , \tag{5.7}$$

where the Liouvillians $L_X$ and $L_Y$

$$L_X \sigma_a = \mu \sigma_a \quad , \tag{5.8}$$

$$L_Y \sigma_a = [\mu, \sigma_a] \quad , \tag{5.9}$$

are introduced in order to simplify the notation. Equation (5.7) is the most condensed and general expression for the absorption profile of an atomic bond on a crystal. We recognize the time regression operator $i/(\omega - L_a + i\Gamma(\omega))$, which is the same indeed as in Eq. (4.1). Initial correlations are accounted for by the frequency-dependent operator $T(\omega)$, which is explicitly

$$T(\omega) \sigma_a = \mathrm{Tr}_p L_{ap} \frac{i}{\omega - L_a - L_p} L_Y \frac{1}{i0^+ - L_a - L_p} L_{ap}(\sigma_a \bar{\rho}_p) \quad . \tag{5.10}$$

Furthermore, we notice that the series of Liouvillians under the trace in Eq. (5.7) act on the stead-state density operator $\bar{\rho}_a$ of the adsorbate, which can be obtained by solving Eq. (4.4).

## VI.  MATRIX ELEMENTS OF $\Gamma(\omega)$ AND $T(\omega)$

Eigenvalues and eigenstates of the atomic-bond Hamiltonian $H_a$ from Eq. (2.2) are defined by

$$H_a|p> = \hbar\omega_p|p> \quad , \tag{6.1}$$

and due to the neglect of lateral motion the eigenvalues $\hbar\omega_p$ are non-degenerate. For realistic adsorbate systems there are approximately 25 bound states $|p>$.  In this section we expand the various Liouvillians onto the set $\{|p>\}$ of adsorbate bound states.

Without coupling to the reservoir $(\Gamma(\omega) = 0, T(\omega) = 0)$ the time regression operator is determined by the inverse of $\omega - L_a$, and with Eq. (6.1) we readily find

$$<p|\{(\omega-L_a)\sigma\}|q> = (\omega-\Delta_{pq}) <p|\sigma|q> \quad , \tag{6.2}$$

in terms of the level separations

$$\Delta_{pq} = \omega_p - \omega_q \quad . \tag{6.3}$$

Equation (6.2) relates the matrix elements of $(\omega-L_a)\sigma$ to the matrix elements of $\sigma$ for any adsorbate density operator $\sigma$, and thus Eq. (6.2) implies the matrix representation of the Liouvillian $\omega - L_a$.

The coupling between the crystal-atom motion and the adsorbate motion is established by the Hamiltonian $H_{ap}$ of Eq. (2.3), which has the adbond part

$$S = \frac{dV}{dz} \quad . \tag{6.4}$$

Matrix elements of this Hermitian operator will be denoted by

$$S_{pq} = \langle p|S|q\rangle = S_{qp}^* \quad . \tag{6.5}$$

Similarly we denote the matrix elements of $\mu$ by $\mu_{pq} = \langle p|\mu|q\rangle = \mu_{qp}^*$. In case of a Morse potential explicit expressions for $S_{pq}$ and $\mu_{pq}$ can be derived, with an integral due to Rosen.[16] Furthermore, we remark that for any potential $V(z)$ the diagonal matrix elements of its derivative vanish with respect to the eigenstates of $H_a$, e.g.,[17]

$$S_{pp} = 0 \quad . \tag{6.6}$$

The permanent dipole moments $\mu_{pp}$ of level $|p\rangle$, however, are finite in general.

With the methods of Ref. 15 we can evaluate the matrix elements of $\Gamma(\omega)$, as defined in Eq. (4.2), with respect to the basis set $\{|p\rangle\}$. The results is

$$\langle p|(\Gamma(\omega)\sigma)|q\rangle = \sum_{ab} \{\tilde{f}(\Delta_{qa}+\omega)S_{pa}S_{ab}\langle b|\sigma|q\rangle + \tilde{f}^*(\Delta_{pa}-\omega)S_{qa}^*S_{ab}^*\langle p|\sigma|b\rangle$$

$$- (\tilde{f}(\Delta_{bp}+\omega)S_{pa}S_{bq} + \tilde{f}^*(\Delta_{aq}-\omega)S_{qb}^*S_{ap}^*)\langle a|\sigma|b\rangle\} \quad , \tag{6.7}$$

in terms of the matrix elements of $S$ and the reservoir correlation function $\tilde{f}(\omega)$ from Section III. It appears that the frequency dependence of $\Gamma(\omega)$ enters as a shift of the level separations $\Delta_{pq}$ in the arguments of the correlation function.

The initial correlation operator $T(\omega)$ from Eq. (5.10) involves the inversion of two Liouvillians. After laborous computations we obtain

$$\langle p|(T(\omega)\sigma)|q\rangle = \sum_{abc} \frac{\mu_{bc}}{\Delta_{cb}+\omega} \{(\bar{f}(\Delta_{qc}) - \bar{f}(\Delta_{qb}+\omega))S_{pb}S_{ca}\langle a|\sigma|q\rangle$$

$$- (\bar{f}*(\Delta_{cq}) - \bar{f}*(\Delta_{bq}-\omega))S_{pb}S_{aq}\langle c|\sigma|a\rangle$$

$$+ (\bar{f}(\Delta_{bp}) - \bar{f}(\Delta_{cp}+\omega))S_{cq}S_{pa}\langle a|\sigma|b\rangle$$

$$- (\bar{f}*(\Delta_{pb}) - \bar{f}*(\Delta_{pc}-\omega))S_{cq}S_{ab}\langle p|\sigma|a\rangle\}$$

$$- \sum_{abc} \frac{\mu_{pc}}{\Delta_{cp}+\omega} \{(\bar{f}(\Delta_{ac}) - \bar{f}(\Delta_{ap}+\omega))S_{aq}S_{cb}\langle b|\sigma|a\rangle$$

$$- (\bar{f}*(\Delta_{ca}) - \bar{f}*(\Delta_{pa}-\omega))S_{aq}S_{ba}\langle c|\sigma|b\rangle\}$$

$$- \sum_{abc} \frac{\mu_{bq}}{\Delta_{qb}+\omega} \{(\bar{f}(\Delta_{ba}) - \bar{f}(\Delta_{qa}+\omega))S_{pa}S_{ac}\langle c|\sigma|b\rangle$$

$$- (\bar{f}*(\Delta_{ab}) - \bar{f}*(\Delta_{aq}-\omega))S_{pa}S_{cb}\langle a|\sigma|c\rangle\} \quad . \tag{6.8}$$

Again, the frequency depenence enters as a shift of the arguments in $\bar{f}(\Delta_{ab})$, but in addition overall factors $(\Delta_{ab}+\omega)^{-1}$ appear. Furthermore, we see that $T(\omega)$ depends on the matrix elements of the dipole operator.


## VII. TWO STATES

With the matrix representations of the various Liouvillians it is straightforward to evaluate $I(\omega)$ from Eq. (5.7) for any configuration of levels, or, for any potential $V(z)$. The profile $I(\omega)$ will exhibit many overlapping lines at the adsorbate resonances $\Delta_{ab}$. In order to disentangle the contributions to

$I(\omega)$ from the different transitions, and to elucidate the significance of initial correlations, we elaborate on the situation where the potential supports only two bound states. Let us denote these states by $|2\rangle$, $|1\rangle$, with the convention that $\omega_o$ $\omega_2 - \omega_1 > 0$. From Eq. (6.5) it follows that $S_{11} = S_{22} = 0$, and therefore the only non-vanishing matrix element of $dV/dz$ is

$$S_o = \langle 1|S|2\rangle \quad , \tag{7.1}$$

which will be assumed to be real (as for a Morse potential).

From Eqs. (6.2) and (6.7) we find the matrix representation of $\omega - L_a + i\Gamma(\omega)$. On the basis $|2\rangle\langle 2|$, $|1\rangle\langle 1|$, $|2\rangle\langle 1|$, $|1\rangle\langle 2|$ this becomes

$$\omega - L_a + i\Gamma(\omega) = $$

$$\begin{pmatrix} \omega + ip(\omega) & -iq(\omega) & 0 & 0 \\ -ip(\omega) & \omega + iq(\omega) & 0 & 0 \\ 0 & 0 & \omega - \omega_o + i\eta(\omega) & -i\eta(\omega) \\ 0 & 0 & -i\eta(\omega) & \omega + \omega_o + i\eta(\omega) \end{pmatrix} \quad , \tag{7.2}$$

in terms of the parameter functions

$$p(\omega) = S_o^2(\tilde{f}(\omega_o + \omega) + \tilde{f}*(\omega_o - \omega)) \quad , \tag{7.3}$$

$$q(\omega) = S_o^2(\tilde{f}(-\omega_o + \omega) + \tilde{f}*(-\omega_o - \omega)) \quad , \tag{7.4}$$

$$\eta(\omega) = S_o^2(\tilde{f}(\omega) + \tilde{f}*(-\omega)) \quad . \tag{7.5}$$

Inversion of the matrix (7.2) then yields the resolvent for $\bar{\rho}_a(\omega)$, Eq. (4.1), and a Fourier-Laplace inverse of the result gives $\rho_a(t)$. Recalling the complicated frequency dependence of $\bar{f}(\omega)$, Section III, shows that an evaluation of $\rho_a(t)$ in the transient regime $0 < t < \infty$ is evidently impossible, unless numerical methods are applied.

Fortunately, the absorption profile depends only on the steady-state density operator $\rho_a(t - \infty)$, which obeys Eq. (4.4). With the matrix representation (7.2) this equation is easily solved, with result

$$\bar{\rho}_a = |2>n_2<2| + |1>n_1<1| \quad . \tag{7.6}$$

The steady-state level populations are

$$n_2 = \frac{q(0)}{p(0) + q(0)} \quad , \quad n_1 = \frac{p(0)}{p(0) + q(0)} \quad , \tag{7.7}$$

and Eq. (7.6) expresses that the coherence $<1|\bar{\rho}_a|2>$ vanishes, as usual in thermal equilibrium. From the definitions of $p(0)$ and $q(0)$ in Eqs. (7.3) and (7.4) we see that the factor $S_o^2$ drops out, and hence the populations are completely determined by the reservoir correlation function $\bar{f}(\omega)$, at the resonance $\omega - \omega_o$. With Eq. (3.6) we then find that the dependence on $\xi$ also disappears, so that $n_2$ and $n_1$ are determined by $g(z)$, which has only the temperature as parameter. Explicitly,

$$n_2 = \frac{\mathrm{Re}\ g(-\omega_o/\omega_D)}{\mathrm{Re}(g(\omega_o/\omega_D) + g(-\omega_o/\omega_D))} \quad , \tag{7.8}$$

$$n_1 = \frac{\mathrm{Re}\ g(\omega_o/\omega_D)}{\mathrm{Re}(g(\omega_o/\omega_D) + g(-\omega_o/\omega_D))} \quad , \tag{7.9}$$

which contain only the real parts of the correlation functions. Then it follows from Eq. (3.10) that for $\omega_0 > \omega_D$ the level populations are undetermined. This is a consequence of the fact that we restricted the atom-crystal interaction to single-phonon couplings.

## VIII. INITIAL CORRELATION OPERATOR

For a two-state system the initial correlation operator $T(\omega)$ is a $4 \times 4$ matrix, but its general representation, as it follows from Eq. (6.8), is still cumbersome. For the evaluation of the spectrum $I(\omega)$, however, we only need to know the result of its action on $\bar{\rho}_a$, as can be seen from Eq. (5.7). Since $\bar{\rho}_a$ has only two non-vanishing matrix elements, rather than four, this simplifies the situation. On the same basis as the representation (7.2), we then find

$$
T(\omega)\bar{\rho}_a = \begin{pmatrix} x(\omega) \\ -x(\omega) \\ y(\omega) \\ -y(\omega) \end{pmatrix} \quad , \tag{8.1}
$$

with

$$
x(\omega) = \frac{S_o^2}{\omega}(\mu_{11}-\mu_{22})
$$

$$
\times \{n_2(\tilde{f}(\omega_o) - \tilde{f}(\omega_o+\omega) - \tilde{f}*(\omega_o) + \tilde{f}*(\omega_o-\omega))
$$

$$
+ n_1(\tilde{f}(-\omega_o) - \tilde{f}(-\omega_o+\omega) - \tilde{f}*(-\omega_o) + \tilde{f}*(-\omega_o-\omega))\} \quad , \tag{8.2}
$$

$$y(\omega) = \frac{2S_o^2}{\omega_o^2 - \omega^2} \mu_{21}$$

$$\times \{n_2((\tilde{f}(\omega_o) - \tilde{f}(\omega))(\omega_o + \omega) + (\tilde{f}*(\omega_o) - \tilde{f}*(-\omega`)(\omega - \omega_o))$$

$$+ n_1((\tilde{f}(-\omega_o) - \tilde{f}(\omega))(\omega_o - \omega) + (\tilde{f}*(-\omega) - \tilde{f}*(-\omega_o))(\omega + \omega_o))\} \quad . \qquad (8.3)$$

The right-most factor in Eq. (5.7) is $(L_\gamma - iT(\omega))\bar{\rho}_a$, and therefore the relative significance of the initial correlations follows from a comparison of $T(\omega)\bar{\rho}_a$ with $L_\gamma\bar{\rho}_a$. With Eq. (5.9) we find

$$L_\gamma\bar{\rho}_a = \mu_{21}(n_1 - n_2) \begin{pmatrix} 0 \\ 0 \\ 1 \\ -1 \end{pmatrix} \quad . \qquad (8.4)$$

The most important difference is that $L_\gamma\bar{\rho}_a$ only depends on the transition dipole matrix element $\mu_{21}$, whereas $T(\omega)$ acquires a contribution from the permanent dipole moments of the two levels (terms proportional to $x(\omega)$). Furthermore, $T(\omega)$ is proportional to $S_o^2$ (the strength of the interaction between the vibrating atom and the crystal), whereas $L_\gamma\bar{\rho}_a$ is independent of this parameter.

IX. <u>LINE SHAPE</u>

An absorption profiel for a two-state system is called a line shape, because it singles out a specific transition of the vibrational bond. With the matrix representations of the previous sections we are now able to construct the line shape $I(\omega)$ by simple matrix operations. First we define the dimensionless line shape $\bar{I}(\omega)$ by

$$\bar{I}(\omega) = I(\omega)\{I_p(\epsilon_o \hbar c)^{-1}|\underline{e}_z \cdot \underline{\epsilon}_L|^2 \mu_{21}^2\}^{-1} \quad , \tag{9.1}$$

in order to suppress irrelevant overall factors. Then we write $\bar{I}(\omega)$ as a sum of two contributions

$$\bar{I}(\omega) = \bar{I}(\omega)_{reg} + \bar{I}(\omega)_{in} \quad , \tag{9.2}$$

where $\bar{I}(\omega)_{reg}$ comes from the term $L_\gamma \bar{\rho}_a$ (regression part) and $\bar{I}(\omega)_{in}$ represent the initial-correlation contribution. It appears that $\bar{I}(\omega)$ can be expressed entirely in the parameters

$$a = \xi S_o^2 \quad , \tag{9.3}$$

$$m = (\frac{\mu_{22} - \mu_{11}}{\mu_{21}})^2 \quad . \tag{9.4}$$

Here, a equals the half width at half maximum if the line would be approximated by a Lorentzian, and in the case $T = 0$, $\omega_o = \frac{1}{2}\omega_D$, and m measures the relative importance of the permanent dipole moments in comparison with the transition dipole moment. We finally obtain

$$\bar{I}(\omega)_{reg} = 2\omega\omega_o(n_1 - n_2) \, \text{Re} \, \frac{i}{D(\omega)_{coh}} \quad , \tag{9.5}$$

$$\bar{I}(\omega)_{in} = 2\omega\omega_o \, \text{Re}\{\frac{i}{D(\omega)_{coh}} \phi(\omega) - \frac{m}{D(\omega)_{pop}} \psi(\omega)\} \quad , \tag{9.6}$$

in terms of the auxiliary functions

$$D(\omega)_{coh} = \omega^2 - \omega_o^2 + 2i\omega\eta(\omega) \quad , \tag{9.7}$$

$$D(\omega)_{pop} = \omega(\omega+i(p(\omega)+q(\omega))) \quad , \tag{9.8}$$

$$\phi(\omega) = -2ia\{n_2(\frac{g(\hat{\omega}_o)-g(\hat{\omega})}{\omega_o-\omega} + \frac{g^*(-\hat{\omega})-g^*(\hat{\omega}_o)}{\omega+\omega_o})$$

$$+ n_1(\frac{g(-\hat{\omega}_o)-g(\hat{\omega})}{\omega_o+\omega} - \frac{g^*(-\hat{\omega}_o)-g^*(-\hat{\omega})}{\omega_o-\omega})\} \quad , \tag{9.9}$$

$$\psi(\omega) = \frac{a}{2\omega_o}\{n_2(g(\hat{\omega}_o) - g(\hat{\omega}_o+\hat{\omega}) - g^*(\hat{\omega}_o) + g^*(\hat{\omega}_o-\hat{\omega}))$$

$$+ n_1(g(-\hat{\omega}_o) - g(-\hat{\omega}_o+\hat{\omega}) - g^*(-\hat{\omega}_o) + g^*(-\hat{\omega}_o-\hat{\omega}))\} \quad , \tag{9.10}$$

with $\hat{\omega} = \omega/\omega_D$ the frequency in units of $\omega_D$. The two $D(\omega)$ functions are the determinants of the two submatrices in Eq. (7.2), and the subscripts coh and pop refer to the subspaces of coherences ($|2\rangle\langle1|$ , $|1\rangle\langle2|$) and populations ($|2\rangle\langle2|$ , $|1\rangle\langle1|$), respectively. The above sequence of formulas determines the shape of a single absorption line, where $\omega_o$, a, $\gamma$ and m are the only arbitrary parameters (if we take $\omega_D$ as the frequency unit). For a specified potential V(z) we can express $\omega_o$, a and m in properties of this potential, and $\gamma$ is simply the temperature of the crystal.

Substitution of $D(\omega)_{coh}$ into Eq. (9.5) and removal of the real part yields

$$\bar{I}(\omega)_{reg} = \frac{4(n_1-n_2)\omega_o\omega^2\text{Re}\eta(\omega)}{\{\omega_o^2-\omega^2+2\omega\text{Im}\eta(\omega)\}^2 + 4\omega^2(\text{Re}\eta(\omega))^2} \quad . \tag{9.11}$$

From the definition (7.5) of $\eta(\omega)$ and the property (3.10) of the reservoir correlation function, it follows that $\mathrm{Re}\,\eta(\omega) = 0$ for $\omega > \omega_D$, and consequently

$$\overline{I(\omega)}_{reg} = 0 \quad , \quad \text{for } \omega > \omega_D \quad . \tag{9.12}$$

Therefore, absorption for $\omega > \omega_D$ can only be a result of nonvanishing initial correlations.

## X. APPROXIMATIONS

Before we discuss the relevance of the finite memory-time in the time regression of dipole correlation functions and the importance of the inclusion of initial correlations, we summarize the results from earlier theories. A most obvious approximation would be the factorization

$$\lim_{t \to \infty} D(0,t) = [\mu,\overline{\rho}_a]\overline{\rho}_p \tag{10.1}$$

of the initial condition for the time-regression equation (5.5). It can be shown[15] that this implies $\overline{T(\omega)} = 0$, and consequently $\overline{I(\omega)}_{in} = 0$, so that $\overline{I(\omega)}$ is approximated by $\overline{I(\omega)}_{reg}$.

A more rigorous simplification is the Markov approximation, in which any memory effect is discarded. First this implies the factorization (10.1), where a memory of $\rho(t)$ to its recent past is neglected. Secondly, we adopt a memoryless description of the time regression, which yields a frequency-independent relaxation operator $\Gamma_m$. The Markovian equivalent of the matrix (7.2) reads[18]

$$\omega - L_a + i\Gamma_m =$$

$$\begin{pmatrix} \omega + ip(0) & -iq(0) & 0 & 0 \\ -ip(0) & \omega + iq(0) & 0 & 0 \\ 0 & 0 & \omega - \omega_o + i\eta(\omega_o) & -i\eta^*(\omega_o) \\ 0 & 0 & -i\eta(\omega_o) & \omega + \omega_o + i\eta^*(\omega_o) \end{pmatrix} \quad . \tag{10.2}$$

In the left-top submatrix, the parameter functions $p(\omega)$ and $q(\omega)$ are replaced by their values at $\omega = 0$. Since the steady-state level populations $n_1$ and $n_2$ are determined by $\Gamma(0)$, we conclude that $n_1$ and $n_2$ are unaffected by this approximation. In the right-bottom submatrix the functions $\eta(\omega)$ are now evaluated at the resonance frequency $\omega_o$, rather than at the laser frequency $\omega$, and furthermore, the functions $\eta(\omega_o)$ in the fourth column are now complex-conjugated. In this approximation the line shape is found to be

$$\overline{I}(\omega)_m = \frac{4(n_1 - n_2)\omega_o\omega^2 \mathrm{Re}\eta(\omega_o)}{\{\omega_o^2 - \omega^2 + 2\omega_o \mathrm{Im}\eta(\omega_o)\}^2 + 4\omega^2(\mathrm{Re}\eta(\omega_o))^2} \quad , \tag{10.3}$$

which greatly resembles $\overline{I}(\omega)_{reg}$ from Eq. (9.11). The most important difference is that we now find $\mathrm{Re}\eta(\omega_o)$ in the numerator, rather than $\mathrm{Re}\eta(\omega)$, which implies that $\overline{I}(\omega)_m$ is finite for $\omega > \omega_D$.

In the most simple theory of relaxation (which leads to a master equation for the time evolution of the populations), we furthermore neglect any coupling between coherences and populations, and between coherences which evolve with a different frequency in a free evolution (no coupling to the reservoir). This approximation is usually called the secular approximation, and it is equivalent to the neglect of terms which oscillate fast on a time scale $1/a$ (Eq. (9.3)).

Then we replace the off-diagonal matrix elements $-i\eta(\omega_0)$ and $-i\eta^*(\omega_0)$ in Eq. (10.2) by zero, which gives for the line shape (s - secular)

$$\overline{I}(\omega)_s = \omega_0(n_1 - n_2) \; \text{Re} \; \frac{i}{\omega - \omega_0 + i\eta(\omega_0)} \quad . \tag{10.4}$$

We obtain the standard Lorentzian, which has its maximum at $\omega = \omega_0 + \text{Im}\eta(\omega_0)$, and has a half-width at half-maximum equal to $\text{Re}\eta(\omega_0)$.

It is easy to verify that the three approximations yield the same value for $\overline{I}(\omega)$ at the resonance frequency $\omega_0$, e.g.,

$$\overline{I}(\omega_0)_{reg} = \overline{I}(\omega_0)_m = \overline{I}(\omega_0)_s = \omega_0(n_1 - n_2) \text{Re} \; \frac{1}{\eta(\omega_0)} \quad . \tag{10.5}$$

Conversely, this implies that the successive refinements will have a major significance in the line wings only, which is illustrated in Fig. 1.

## XI. RESULTS

The line shape $\overline{I}(\omega)$ is composed of two contributions, which are drawn separately in Fig. 2 for a specific set of parameters. We notice that the initial correlation part is not small, and that it takes on both positive and negative values. A considerable increase of the absorption is found in the line center and the red wing, whereas the blue wing is only slightly modified, both in comparison with the line shape $\overline{I}(\omega)_{reg}$ (the best approximation so far). Due to the neglect of permanent dipole moments in this case ($m = 0$), we find a sharp edge at $\omega = \omega_D$, and a vanishing absorption for $\omega > \omega_D$. Of course, multiphonon processes would also give rise to absorption at $\omega > \omega_D$, but these contributions are assumed to be small. The cutoff can be understood from the fact that a photon absorption from the laser gives rise to a transition $|1> \rightarrow |2>$ of the adsorbate. Energy

conservation then implies that this process must be followed by a single-phonon emission into the crystal, under a decay $|2> \rightarrow |1>$ of the adsorbate bond. In a Debye model there are no phonon modes available for $\omega > \omega_D$, and therefore this process cannot occur.

A remarkable profile arises if we allow the atomic bond to have a permanent dipole moment ($m \neq 0$), which is illustrated in Fig. 3. For $\omega < \omega_D$ the value of $m$ has hardly any significance, but above the cutoff frequency we now find a finite absorption if $m \neq 0$. We observe a peak at $\omega - \omega_0 + \omega_D$, a smooth background for $\omega_D < \omega < \omega_0 + \omega_D$. How can this be understood? First we remember that a low-intensity profile is a balance between the stimulated absorption and emission rates for single-photon transitions. Hence the phenomenon cannot be attributed to multiphoton processes. Then we recall that we restricted ourselves to a model of single-phonon interactions, which rules out multiphonon processes. Third, a positive $I(\omega)$ corresponds to a photon absorption. A positive $I(\omega)$ in the range $\omega > \omega_D > \omega_0$ can then only be found from the following energy-conserving process. Initially the adsorbate is in its lower state $|1>$. Absorption of a photon then excites the system to a virtual level with energy $\hbar\omega$ above the energy of state $|1>$, and subsequently this state decays to $|2>$, accompanied by the emission of a phonon with frequency $\omega - \omega_0$. The second transition can only occur if $\omega - \omega_0 < \omega_D$, or $\omega < \omega_0 + \omega_D$. This explains why $I(\omega)$ vanishes identically for $\omega > \omega_0 + \omega_D$, and can be finite for $\omega_D < \omega < \omega_0 + \omega_D$.

## XII. CONCLUSIONS

We performed very detailed calculations on the optical spectral profile and line shapes of physisorbed atoms on the surface of a harmonic crystal. Coupling of the atomic motion to the phonon field of the crystal provides the relaxation mechanism for the evolution of the adsorbate vibrational states towards thermal

equilibrium. Since the amplitude correlation function of a substrate atom has a finite decay time, the time evolution of the reduced adsorbate density operator exhibits a memory effect. The absorption profile is determined by dipole correlation functions, depending on two times. We identified two different aspects of the memory, which were called regression and initial correlation. A general finite memory·time reservoir theory was applied for the evaluation of the line shape.

It appeared that the properties of the reservoir could be accounted for by a single dimensionless function $g(z)$, which has only the dimensionless temperature $\gamma$ as parameter (apart from a scaling factor $\xi$). The other parameters of the line shape are the resonance frequency $\omega_o$ of the uncoupled adsorbate, the interaction-strength parameter a (frequency, related to line width), and the permanent-dipole parameter m (dimensionless). From our analytical expression for the line shape we showed that any absorption above the Debye frequency can only be a consequence of nonvanishing initial correlations (in the single-phonon approximation). It was exemplified (Fig. 3) that $I(\omega)$ is finite indeed for $\omega > \omega_D$, provided that the transition has a permanent dipole moment (as is the case for a Morse potential).

## ACKNOWLEDGMENTS

## REFERENCES

1. Z. W. Gortel, P. Piercy, R. Teshima and H. J. Kreuzer, Surf. Sci. 165, L12 (1986).

2. Z. W. Gortel, P. Piercy, R. Teshima and H. J. Kreuzer, Surf. Sci. 166, L199 (1986).

3. Z. W. Gortel, P. Piercy, R. Teshima and H. J. Kreuzer, Surf. Sci. 179, 176 (1987).

4. J. C. Ariyasu, D. L. Mills, K. G. Lloyd and J. C. Hemminger, Phys. Rev. B 28, 6123 (1983).

5. B. N. J. Persson, J. Phys. C 17, 4741 (1984).

6. J. C. Tully, Y. J. Chabal, K. Raghavachari, J. M. Bowman and R. R. Lucchese, Phys. Rev. B 31, 1184 (1985).

7. H. Metiu and W. E. Palke, J. Chem. Phys. 69, 2574 (1978).

8. B. N. J. Persson and R. Ryberg, Phys. Rev. B 24, 6954 (1981).

9. R. Ryberg, Phys. Rev. B 32, 2671 (1985).

10. G. Nienhuis, Physica 66, 245 (1973).

11. A. A. Maradudin, E. W. Montroll, G. H. Weiss and I. P. Ipatova, Theory of Lattice Dynamics in the Harmonic Approximation, Suppl. 3 of Solid State Physics (Academic, New York, 1971).

12. W. H. Louisell, Quantum Statistical Properties of Radiation (Wiley, New York, 1973).

13. H. F. Arnoldus, S. van Smaalen and T. F. George, Adv. Chem. Phys. (1987), in press.

14. H. F. Arnoldus and T. F. George, Phys. Rev. B 36, 2987 (1987).

15. H. F. Arnoldus and T. F. George, J. Math. Phys. 28, 2731 (1987).

16. N. Rosen, J. Chem. Phys. 1, 319 (1933).

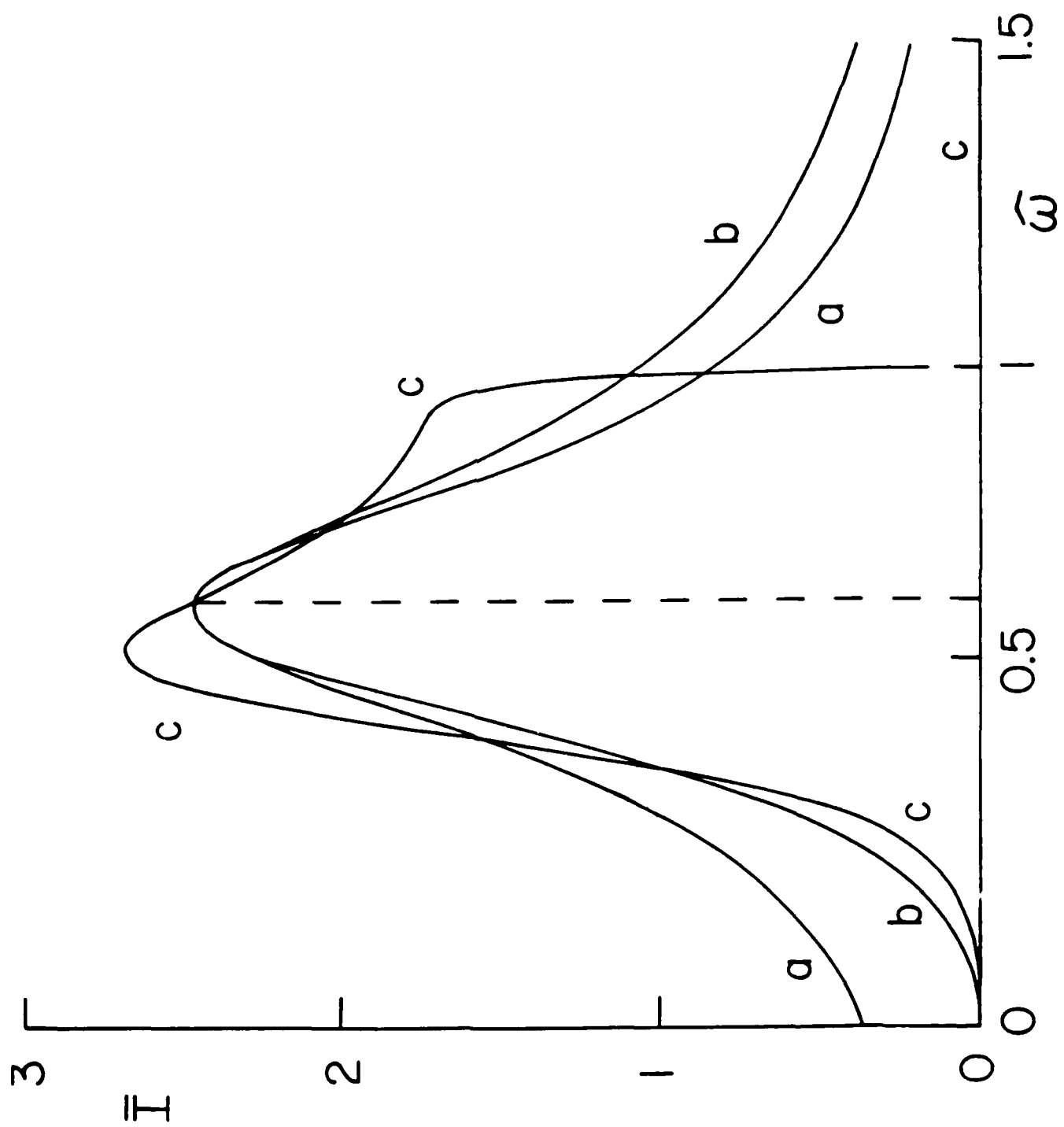17. E. Merzbacher, Quantum Mechanics (Wiley, New York, 1961), p. 41.

18. H. F. Arnoldus and T. F. George, Phys. Rev. B $\underline{35}$, 5955 (1987).

FIGURE CAPTIONS

Fig. 1. Secular (a), Markov (b) and regression (c) approximation of $\overline{I}(\omega)$ as a function of $\hat{\omega} = \omega/\omega_D$, and for $\omega_o = 0.65 \times \omega_D$ (dotted line), $a = 0.4 \times \omega_D$, $\gamma = 10$ (low temperature) and $m = 0$. Curve a is a Lorentzian around $\omega_o + \text{Im}\eta(\omega_o)$, but for the present parameters the line shift is negligible ($\text{Im}\eta(\omega_o) = -0.011$). As predicted in Eq. (10.5), the value of $\overline{I}(\omega_o)$ is the same for the three curves. The secular approximation gives a finite absorption for $\omega \sim 0$, whereas the improved results, curves b and c, give a vanishing absorption for $\omega \to 0$. In the blue wing, however, curves a and b remain finite, but the most refined theory gives $I(\omega) = 0$ for $\omega > \omega_D$.

Fig. 2. Curve a and b are $\overline{I}(\omega)_{reg}$ and $\overline{I}(\omega)_{in}$, respectively, for the same parameters as in Fig. 1. Their sum, curve c, is $\overline{I}(\omega)$, which is calculated with the present theory. Comparison of curves a and c shows the significance of the improvement. Note also the considerable red shift of the line with respect to the resonance frequency $\omega_o$.

Fig. 3. Curve a is the same as curve c from Fig. 2 ($m = 0$), and for curve b we took the dipole-moment parameter $m$ equal to 0.7. The nonzero value of $m$ appears to have no importance at all for $\omega < \omega_D$, but for $\omega > \omega_D$ only the profile b remains finite. As pointed out in the text, the absorption for $\omega > \omega_D$ is entirely due to the initial correlations.
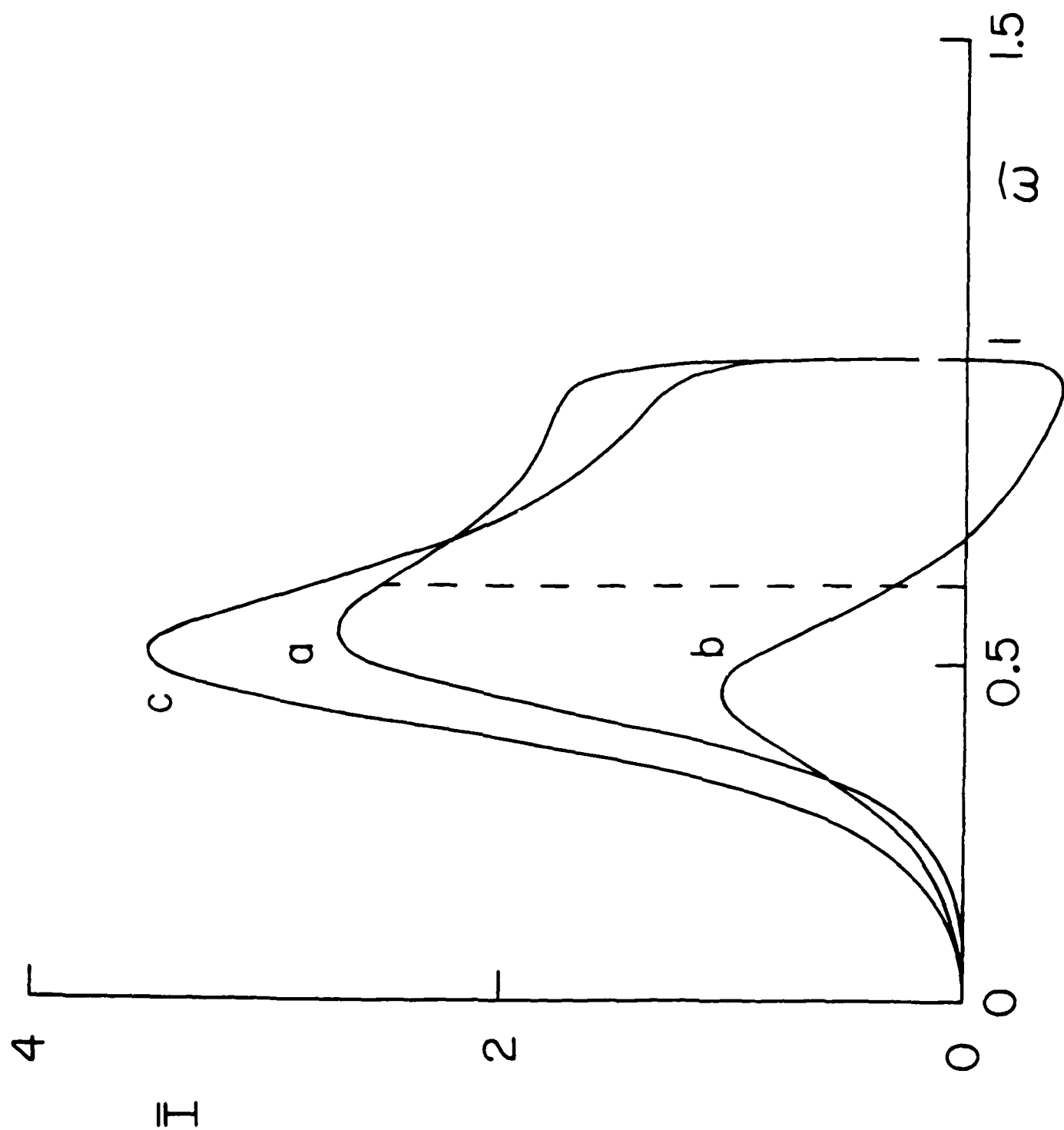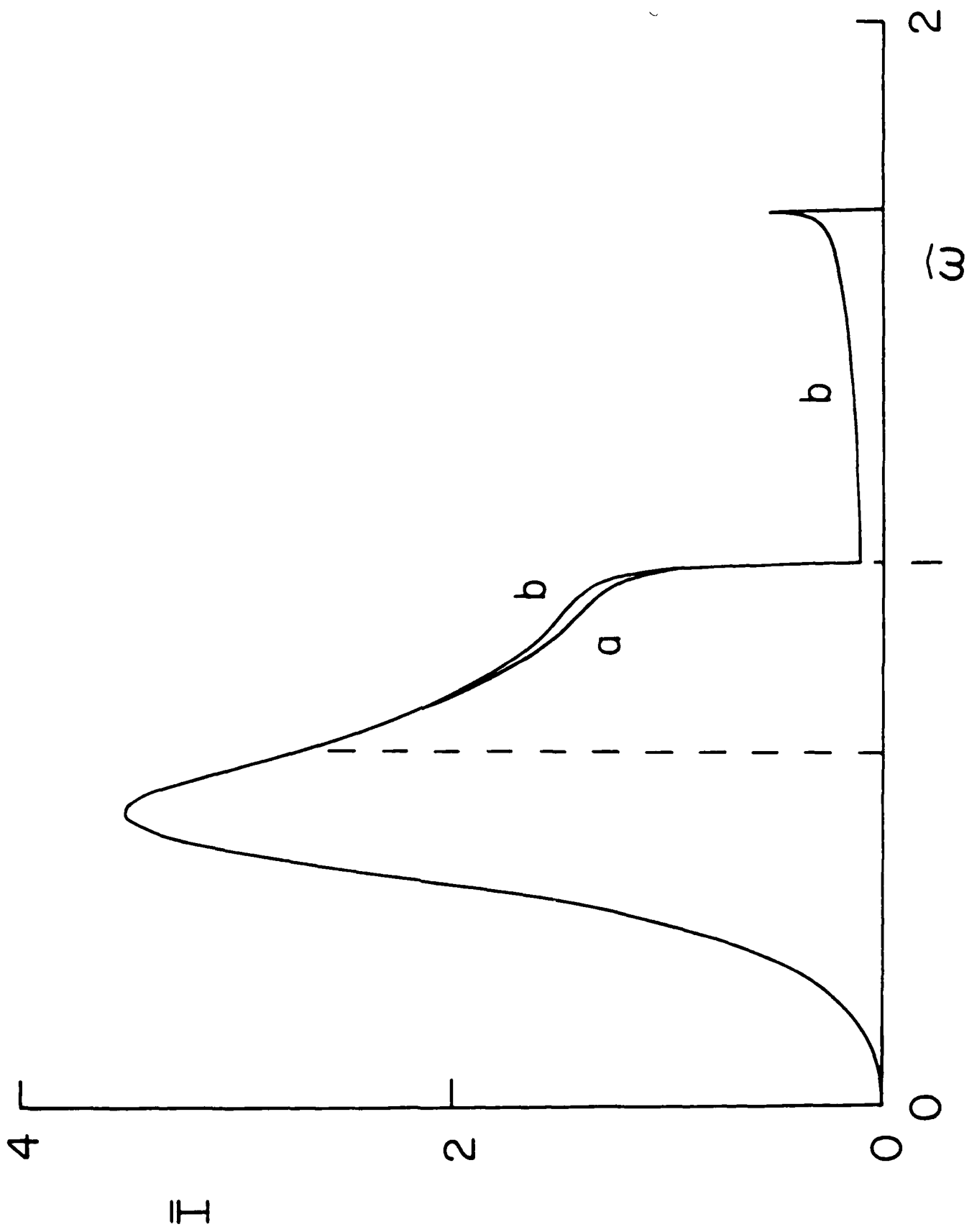
Fig. 1

$\bar{I}$

3

2

1

0

0        0.5        1        1.5

$\hat{\omega}$

a
b
c

Fig. 2

Fig. 3

## TECHNICAL REPORT DISTRIBUTION LIST, GEN

| | No. Copies | | No. Copies |
|---|---|---|---|
| Office of Naval Research<br>Attn: Code 1113<br>800 N. Quincy Street<br>Arlington, Virginia 22217-5000 | 2 | Dr. David Young<br>Code 334<br>NORDA<br>NSTL, Mississippi 39529 | 1 |
| Dr. Bernard Douda<br>Naval Weapons Support Center<br>Code 50C<br>Crane, Indiana 47522-5050 | 1 | Naval Weapons Center<br>Attn: Dr. Ron Atkins<br>Chemistry Division<br>China Lake, California 93555 | 1 |
| Naval Civil Engineering Laboratory<br>Attn: Dr. R. W. Drisko, Code L52<br>Port Hueneme, California 93401 | 1 | Scientific Advisor<br>Commandant of the Marine Corps<br>Code RD-1<br>Washington, D.C. 20380 | 1 |
| Defense Technical Information Center<br>Building 5, Cameron Station<br>Alexandria, Virginia 22314 | 12<br>high<br>quality | U.S. Army Research Office<br>Attn: CRD-AA-IP<br>P.O. Box 12211<br>Research Triangle Park, NC 27709 | 1 |
| DTNSRDC<br>Attn: Dr. H. Singerman<br>Applied Chemistry Division<br>Annapolis, Maryland 21401 | 1 | Mr. John Boyle<br>Materials Branch<br>Naval Ship Engineering Center<br>Philadelphia, Pennsylvania 19112 | 1 |
| Dr. William Tolles<br>Superintendent<br>Chemistry Division, Code 6100<br>Naval Research Laboratory<br>Washington, D.C. 20375-5000 | 1 | Naval Ocean Systems Center<br>Attn: Dr. S. Yamamoto<br>Marine Sciences Division<br>San Diego, California 91232 | 1 |
| | | Dr. David L. Nelson<br>Chemistry Division<br>Office of Naval Research<br>800 North Quincy Street<br>Arlington, Virginia 22217 | 1 |

ABSTRACTS DISTRIBUTION LIST, 056/625/629

Dr. J. E. Jensen
Hughes Research Laboratory
3011 Malibu Canyon Road
Malibu, California 90265

Dr. J. H. Weaver
Department of Chemical Engineering
  and Materials Science
University of Minnesota
Minneapolis, Minnesota 55455

Dr. A. Reisman
Microelectronics Center of North Carolina
Research Triangle Park, North Carolina
    27709

Dr. M. Grunze
Laboratory for Surface Science and
      Technology
University of Maine
Orono, Maine 04469

Dr. J. Butler
Naval Research Laboratory
Code 6115
Washington D.C. 20375-5000

Dr. L. Interante
Chemistry Department
Rensselaer Polytechnic Institute
Troy, New York 12181

Dr. Irvin Heard
Chemistry and Physics Department
Lincoln University
Lincoln University, Pennsylvania 19352

Dr. K.J. Klaubunde
Department of Chemistry
Kansas State University
Manhattan, Kansas 66506

Dr. C. B. Harris
Department of Chemistry
University of California
Berkeley, California 94720

Dr. F. Kutzler
Department of Chemistry
Box 5055
Tennessee Technological University
Cookesville, Tennessee 38501

Dr. D. DiLella
Chemistry Department
George Washington University
Washington D.C. 20052

Dr. R. Reeves
Chemistry Department
Renssaeler Polytechnic Institute
Troy, New York 12181

Dr. Steven M. George
Stanford University
Department of Chemistry
Stanford, CA 94305

Dr. Mark Johnson
Yale University
Department of Chemistry
New Haven, CT 06511-8118

Dr. W. Knauer
Hughes Research Laboratory
3011 Malibu Canyon Road
Malibu, California 90265

ABSTRACTS DISTRIBUTION LIST, 056/625/629

Cr. G. A. Somorjai
Department of Chemistry
University of California
Berkeley, California  94720

Dr. J. Murday
Naval Research Laboratory
Code 6170
Washington, D.C.  20375-5000

Dr. J. B. Hudson
Materials Division
Rensselaer Polytechnic Institute
Troy, New York  12181

Dr. Theodore E. Madey
Surface Chemistry Section
Department of Commerce
National Bureau of Standards
Washington, D.C.  20234

Dr. J. E. Demuth
IBM Corporation
Thomas J. Watson Research Center
P.O. Box 218
Yorktown Heights, New York  10598

Dr. M. G. Lagally
Department of Metallurgical
  and Mining Engineering
University of Wisconsin
Madison, Wisconsin  53706

Dr. R. P. Van Duyne
Chemistry Department
Northwestern University
Evanston, Illinois  60637

Dr. J. M. White
Department of Chemistry
University of Texas
Austin, Texas  78712

Dr. D. E. Harrison
Department of Physics
Naval Postgraduate School
Monterey, California  93940

Dr. R. L. Park
Director, Center of Materials
  Research
University of Maryland
College Park, Maryland  20742

Dr. W. T. Peria
Electrical Engineering Department
University of Minnesota
Minneapolis, Minnesota  55455

Dr. Keith H. Johnson
Department of Metallurgy and
  Materials Science
Massachusetts Institute of Technology
Cambridge, Massachusetts  02139

Dr. S. Sibener
Department of Chemistry
James Franck Institute
5640 Ellis Avenue
Chicago, Illinois  60637

Dr. Arnold Green
Quantum Surface Dynamics Branch
Code 3817
Naval Weapons Center
China Lake, California  93555

Dr. A. Wold
Department of Chemistry
Brown University
Providence, Rhode Island  02912

Dr. S. L. Bernasek
Department of Chemistry
Princeton University
Princeton, New Jersey  08544

Dr. W. Kohn
Department of Physics
University of California, San Diego
La Jolla, California  92037

ABSTRACTS DISTRIBUTION LIST, 056/625/629

Dr. F. Carter
Code 6170
Naval Research Laboratory
Washington, D.C.  20375-5000

Dr. Richard Colton
Code 6170
Naval Research Laboratory
Washington, D.C.  20375-5000

Dr. Dan Pierce
National Bureau of Standards
Optical Physics Division
Washington, D.C.  20234

Dr. R. Stanley Williams
Department of Chemistry
University of California
Los Angeles, California  90024

Dr. R. P. Messmer
Materials Characterization Lab.
General Electric Company
Schenectady, New York  22217

Dr. Robert Gomer
Department of Chemistry
James Franck Institute
5640 Ellis Avenue
Chicago, Illinois  60637

Dr. Ronald Lee
R301
Naval Surface Weapons Center
White Oak
Silver Spring, Maryland  20910

Dr. Paul Schoen
Code 6190
Naval Research Laboratory
Washington, D.C.  20375-5000

Dr. John T. Yates
Department of Chemistry
University of Pittsburgh
Pittsburgh, Pennsylvania  15260

Dr. Richard Greene
Code 5230
Naval Research Laboratory
Washington, D.C.  20375-5000

Dr. L. Kesmodel
Department of Physics
Indiana University
Bloomington, Indiana  47403

Dr. K. C. Janda
University of Pittsburg
Chemistry Building
Pittsburg, PA  15260

Dr. E. A. Irene
Department of Chemistry
University of North Carolina
Chapel Hill, North Carolina  27514

Dr. Adam Heller
Bell Laboratories
Murray Hill, New Jersey  07974

Dr. Martin Fleischmann
Department of Chemistry
University of Southampton
Southampton 509 5NH
UNITED KINGDOM

Dr. H. Tachikawa
Chemistry Department
Jackson State University
Jackson, Mississippi  39217

Dr. John W. Wilkins
Cornell University
Laboratory of Atomic and
 Solid State Physics
Ithaca, New York  14853

ABSTRACTS DISTRIBUTION LIST, 056/625/629

Dr. R. G. Wallis
Department of Physics
University of California
Irvine, California 92664

Dr. D. Ramaker
Chemistry Department
George Washington University
Washington, D.C. 20052

Dr. J. C. Hemminger
Chemistry Department
University of California
Irvine, California 92717

Dr. T. F. George
Chemistry Department
University of Rochester
Rochester, New York 14627

Dr. G. Rubloff
IBM
Thomas J. Watson Research Center
P.O. Box 218
Yorktown Heights, New York 10598

Dr. Horia Metiu
Chemistry Department
University of California
Santa Barbara, California 03106

Dr. W. Goddard
Department of Chemistry and Chemical
    Engineering
California Institute of Technology
Pasadena, California 91125

Dr. P. Hansma
Department of Physics
University of California
Santa Barbara, California 93106

Dr. J. Baldeschwieler
Department of Chemistry and
    Chemical Engineering
California Institute of Technology
Pasadena, California 91125

Dr. J. T. Keiser
Department of Chemistry
University of Richmond
Richmond, Virginia 23173

Dr. R. W. Plummer
Department of Physics
University of Pennsylvania
Philadelphia, Pennsylvania 19104

Dr. E. Yeager
Department of Chemistry
Case Western Reserve University
Cleveland, Ohio 41106

Dr. N. Winograd
Department of Chemistry
Pennsylvania State University
University Park, Pennsylvania 16802

Dr. Roald Hoffmann
Department of Chemistry
Cornell University
Ithaca, New York 14853

Dr. A. Steckl
Department of Electrical and
    Systems Engineering
Rensselaer Polytechnic Institute
Troy, New York 12181

Dr. G.H. Morrison
Department of Chemistry
Cornell University
Ithaca, New York 14853

9

END

DATE
FILMED

4-88

DTIC